# BATHYMETRY FROM PLANET SCOPE IMAGERY USING RANDOM FOREST AND DEEP LEARNING

Tatsuyuki Sagawa*[1], Masanao Sumiyoshi[2], Honami Watanabe[3] and Yuta Yamashita[4]
[1] Associate Professor, Faculty of Environmental Studies, Tottori University of Environmental Studies
1-1-1, Wakabadai-kita, Tottori, Tottori 689-1111, Japan
Email: sagawa-t@kankyo-u.ac.jp

[2] Senior Research Officer, Hydrographic and Oceanographic Department, Japan Coast Guard
3-1-1, Kasumigaseki, Chiyoda-ku, Tokyo 100-8932, Japan
Email: msumiyoshi@jodc.go.jp

[3]Researcher, Remote Sensing Technology Center of Japan
TOKYU REIT Toranomon Bldg. 3F, 3-17-1 Toranomon, Minato-ku, Tokyo, 105-0001, Japan
Email: watanabe_honami@restec.jp

[4] Senior Researcher, Bestmateria
2-43-15, Misawa, Hino-shi, Tokyo, 191-0032, Japan
Email: yamashita@b-mat.co.jp

**KEY WORDS:** bathymetry, PlanetScope, deep learning, random forest

**ABSTRACT:** The bathymetry of shallow waters is important for avoiding stranding during navigation. It is also indispensable for analyzing coastal areas because it has large effects on ocean currents and organism habitats. Water depth estimated from satellite images is called as satellite derived bathymetry (SDB), which has been the topic of much study. However, the accuracy of SDB can still be improved. High-spatial-resolution satellite images are now available and image analysis technology using machine learning has been improved. The current study used PlanetScope satellite images (PlanetLabs) with 3-m spatial resolution. We created water depth estimation models using random forest (RF) and deep neural network (DNN) methods. As truth data, LiDAR data for Hateruma, Japan and Oahu, USA were used. The performance of the depth estimation models was evaluated using root mean square error (RMSE) values derived by comparing the estimated depth and LiDAR depth data. We also verified the influence of the surrounding pixels in the input data on water depth estimation, the number of wavelength bands of satellite data, and the selection of data used for model training and verification of the accuracy of SDB. There was little difference in accuracy between RF and DNN. We were able to show that the error can be reduced by including surrounding pixels in the input data, increasing the number of bands, or selecting training and validation data. The water depth estimation accuracy of SDB obtained by the method proposed here was high compared with previous research.

## 1. INTRODUCTION

Shallow water bathymetry is essential information for nautical navigation, tide and wave simulation, and coastal ecosystem analysis. Bathymetry data for shallow waters are required worldwide. The General Bathymetric Chart of the Oceans provide bathymetry data that cover the entire world in a 15-second grid (approximately 450 m at the equator). However, water depth can vary significantly over a horizontal distance of 100 m, necessitating higher-resolution grid data, such as 10 m. Most bathymetry data are derived from satellite-borne altimeter recordings and it is difficult to improve the spatial resolution of these data. Current hydrographic surveying methods include acoustic sounding and airborne light detection and ranging (LiDAR). Acoustic sounding uses survey boats and is inefficient and potentially dangerous in shallow water. LiDAR is suitable for shallow water but requires a flyable area. Both these methods are expensive and data are limited for some regions. Satellite-derived bathymetry (SDB) is another measurement method that uses data recorded by a satellite-borne optical sensor. The technology differs from that of an altimeter. This study focused on SDB technology. In the following, satellite imagery or satellite data refers to data obtained by optical sensors.

Various models have been developed to relate satellite data and water depth. Lee et al. (1998; 1999) proposed a method that explains the relationship between satellite data and water depth based on a radiative transfer model. Theirs is one of the most sophisticated physics-based models. However, it includes many unknown parameters, and the number of parameters should be reduced based on the assumptions used to estimate depth from satellite data. Lyzenga et al. (2006) introduced a simple optical model and proposed a multiple regression equation to relate satellite data and water depth. However, this model also makes assumptions to reduce parameters, such as not considering the effects of scattered light in water.

Satellites observe the radiance from the surface of the earth, which is affected by various factors other than water depth. The information from satellite sensors using several bands is limited and insufficient to estimate all underwater parameters, such as the absorption coefficients of water components and the reflectance of the ocean floor. To increase the amount of information obtained from satellite data, it is possible to use pixels surrounding the target pixel to estimate water depth, or to use satellite images acquired at multiple times. However, the relationship with water depth and other parameters becomes more complex as the amount of input information increases and it becomes difficult to explain physically.

Machine learning is considered effective for relating input data to depth data. Random forest (RF) methods have already been used to create a depth estimation model that performs well (Manessa et al. 2016; Sagawa et al. 2019). Recently, there has been remarkable progress in deep learning, which is also attracting attention in remote sensing research. However, only a few deep neural network (DNN) studies have examined SDB. Therefore, we used a DNN to create a depth estimation model and compared the performance of models based on RF and DNN. We also verified the influence of the surrounding pixels on estimates of water depth, the number of wavelength bands of satellite data, and the selection of data used for training and verification of the accuracy of SDB.

## 2. STUDY AREAS AND DATA

The study areas were Hateruma in Okinawa, Japan and Oahu in Hawaii, USA. The transparency of water in these area is high and bathymetry data measured using LiDAR are available. Table 1 summarizes the bathymetry data, which are very accurate and generally correspond to the Category Zone of Confidence (ZOC) A1 for depth and positioning accuracies defined by the International Hydrographic Organization (IHO) S-67 (IHO, 2020), except for seafloor coverage conditions. These bathymetry data were used as reference data in this study. The bathymetry data for Hateruma were provided by the Hydrographic and Oceanographic Department (JHOD), Japan Coast Guard (JCG) and the data for Oahu were from the National Oceanic and Atmospheric Administration (NOAA).

PlanetScope satellite images (PlanetLabs) with 3-m spatial resolution were used as optical satellite data (Table 3). PlanetScope data are collected by > 100 satellites and the frequency of observation is relatively high for high-spatial-resolution satellite images. The eight band products of PlanetScope are available from August 2021.

**Table 1.** List of reference bathymetry data for the two study areas in Japan and the USA. The stated data accuracy expresses the maximum allowable uncertainty at the 95% confidence interval (CI) with depth z.

| **Area Name** | Hateruma | Oahu |
|---|---|---|
| **Country** | Japan | USA |
| **Provider** | JHOD | NOAA |
| **Measurement method** | ALB | ALB |
| **System** | CZMIL (Teledyne Optech) | CZMIL (Teledyne Optech) |
| **Observation date** | Feb, 2015 | 11 Sep, 2013 |
| **Depth accuracy (m)** | $\pm\sqrt{0.5^2 + (0.013z)^2}$ | $\pm\sqrt{0.20^2 + (0.013z)^2}$ |
| **Positioning accuracy (m)** | 5 + 0.05z | 3.5 + 0.05z |

**Table 2.** Positioning and depth accuracies of ZOC Categories defined by IHO S-67 (IHO, 2020). The stated data accuracy expresses the maximum allowable uncertainty at the 95% confidence interval (CI) with depth z.

| ZOC | Positioning Accuracy (m) | Depth Accuracy (m) |
|---|---|---|
| A1 | ±(5 + 0.05z) | ±(0.5 + 0.01z) |
| A2 | ±20 | ±(1.0 + 0.02z) |
| B | ±50 | ±(1.0 + 0.02z) |
| C | ±500 | ±(2.0 + 0.05z) |
| D | Worse than C | Worse than C |

**Table 3.** List of PlanetScope data for the two study areas in Japan and the USA.

| Site | Date | Number of bands |
|---|---|---|
| Hateruma | 17 Oct 2017 | 4 |
| Oahu | 5 Sep2017 | 4 |
| Hateruma | 10 Mar 2023 | 8 |

## 3. METHODS

Depth estimation models were created using RF and DNN, and the performance of the two models was compared. We also verified the influence of the surrounding pixels in input data on estimates of water depth. At Hateruma, we also compared the results obtained using four- and eight-band satellite images. Furthermore, the selection of training and validation data considered the variation in water depth within a pixel. Details of each process are described below.

### 3.1 Machine learning models

Google Earth Engine (GEE) and Google Colaboratory (GC) (Google, Mountain View, CA, USA) were used for the satellite image analysis and machine learning. GEE is a cloud-based geographical information analysis system and the application programming interface (API) is available in Python and JavaScript. The GEE API includes several machine learning libraries, including an RF regression model. The RF regression model was trained to estimate depth from satellite data on GEE. The number of decision trees to be created was set as 10.

TensorFlow and Keras are open-source libraries for machine learning and artificial neural networks that can be used with GC. A DNN regression model for depth estimation was created in GC. The outlines of the layers are described in Table 4. The input data were radiance values from a single pixel or from 3 × 3 pixels. Each radiance value has four dimensions corresponding to the four wavelength bands. In the DNN model learning process, the optimizer was Adam, the loss function was the mean squared error, and the number of epochs was 10. The numbers of dense layers, neurons in each layer, and epochs were decided through trial and error.

**Table 4.** Layers for the DNN model.

| Layer | Number of input parameters /number of neurons | Activation Function |
|---|---|---|
| Input | 4 (1 x 4) / 36 (3 x 3 x 4) | |
| Dense Layer 1 | 1024 | ReLU |
| Dense Layer 2 | 512 | ReLU |
| Dense Layer 3 | 256 | ReLU |
| Dense Layer 4 | 256 | ReLU |
| Dense Layer 5 | 256 | ReLU |
| Dense Layer 6 | 256 | ReLU |
| Dense Layer 7 | 256 | ReLU |
| Dense Layer 8 | 128 | ReLU |
| Dense Layer 9 | 64 | ReLU |
| Output | 1 | |

### 3.2 Data selection

The satellite and bathymetry data were correlated using horizontal position information. Each pixel of a satellite image has a space corresponding to its resolution. The bathymetry data used as the reference were originally point data. Therefore, the spatial average value of the bathymetry data included in the space of each pixel of satellite data was calculated and associated with the satellite data. However, there is variation in water depth even within the space of each pixel. Since the water depth changes rapidly at the edge of a coral reef, even a 3 × 3 m area may not be uniform. When estimating the water depth for each pixel, the variation in water depth within a pixel can be regarded as error. Therefore, data with high variation should not be used for model building or accuracy verification. The Oahu bathymetry data were obtained as image data from the NOAA website, while the original point data for Hateruma were obtained from the JHOD, making detailed analysis possible.

Data selection Method 1 excludes data where the standard deviation of water depth for each pixel exceeds a threshold, which was set to 0.2 m to exceed the accuracy of the water depth of A1 in ZOC, which is approximately 0.5 m with a 95% confidence interval. In an actual analysis, however, the original data are not necessarily available, such as the Oahu data, and it may not be possible to calculate the variation in the data for each pixel. Therefore, in Method 2, the standard deviation of water depth was calculated from 3 × 3 pixel data, and data with a standard deviation above a threshold of 0.2 m, the same as in Method 1, were excluded.

### 3.3 Machine leaning and accuracy evaluation

As a first step, an analysis based on the conditions listed in Table 5 was conducted to compare the performance of machine learning models with different input data. In this analysis, for both Hateruma and Oahu, the accuracy was highest when 3 × 3 pixel data were used as the input and RF was selected as the machine learning model. Further details are explained in the Results and Discussion.

Based on the initial analysis results, an analysis with the conditions listed in Table 6 was conducted as a second step to assess how much the accuracy can be improved by increasing the number of bands, and to confirm the effect of selecting the bathymetry data used for machine learning and accuracy evaluation.

**Table 5.** List of the initial analysis patterns.

| No | Site | Data | Input | Model |
|---|---|---|---|---|
| 1 | Hateruma | Planet Scope in 2017 | single pixel | RF |
| 2 | Hateruma | Planet Scope in 2017 | single pixel | DNN |
| 3 | Hateruma | Planet Scope in 2017 | 3 x 3 pixels | RF |
| 4 | Hateruma | Planet Scope in 2017 | 3 x 3 pixels | DNN |
| 5 | Oahu | Planet Scope in 2017 | single pixel | RF |
| 6 | Oahu | Planet Scope in 2017 | single pixel | DNN |
| 7 | Oahu | Planet Scope in 2017 | 3 x 3 pixels | RF |
| 8 | Oahu | Planet Scope in 2017 | 3 x 3 pixels | DNN |

**Table 6.** List of the second analysis patterns.

| No | Site | Data | Input | Model | Data Selection |
|---|---|---|---|---|---|
| 9 | Hateruma | Planet Scope in 2023 | 3 x 3 pixels | RF | |
| 10 | Hateruma | Planet Scope in 2023 | 3 x 3 pixels | RF | Data selected by Method 1 |
| 11 | Hateruma | Planet Scope in 2023 | 3 x 3 pixels | RF | Data selected by Method 2 |
| 12 | Hateruma | Planet Scope in 2017 | 3 x 3 pixels | RF | Data selected by Method 2 |
| 13 | Oahu | Planet Scope in 2017 | 3 x 3 pixels | RF | Data selected by Method 2 |

## 4. RESULTS AND DISCUSSION

Table 7 shows the accuracy results corresponding to the run numbers in Table 5. Root mean square error (RMSE) was calculated for both training and validation data. In machine learning, the error for training data is generally smaller than that for validation data. However, because the water depth interval of the validation data was narrow here, the error in the validation data is not necessarily larger than that in the training data. Regarding the input data, the error is clearly smaller when using 3 × 3 pixels than when using a single pixel. For the machine learning models, the error of RF was slightly smaller than that of DNN, although DNN uses more data for learning than RF. However, the difference is slight and can be considered to be at the same level.

Table 8 shows the accuracy results corresponding to the run numbers in Table 6. During validation, RMSE was calculated for depth ranges of 0–10 m and 0–20 m. Comparing the results for No. 9 using 2023 data and No. 3 using 2017 data at Hateruma, the RMSE at depths of 0–20 m is reduced significantly from 1.85 to 1.38 m. This might be largely due to the increase in the number of bands from four to eight. Comparing No. 9 and 10, the error of No. 10 is clearly smaller than that of No. 9, indicating the effect of data selection. Although the error of No. 11 is slightly larger than that of No. 10, it is clearly smaller than that of No. 9. In other words, the effect seen with Method 1 is confirmed with Method 2. Comparison of Nos. 12 and 3, and of Nos. 13 and 7, confirmed that the error is smaller due to the data selection effect of Method 2.

The RMSEs of Nos. 10 and 11 at the water depth of 0–10 m are within depth accuracy of ZOC A2, while the RMSEs at 0–20 m are within depth accuracy of C. The RMSEs of Nos. 12 and 13 in the water depth ranges of 0–10 m and 0–20 m are within depth accuracy of ZOC C. Although the water depth error of Nos. 12 and 13 in the range of 0–10 m is slightly larger than the standard for ZOC A2 and B, it is expected increasing the number of bands will reduce the error, as in No. 11.

Figure 1 shows the reference bathymetry data and SDBs for Nos. 10 and 12 for Hateruma. Figure 2 shows the reference bathymetry data and SDB for No. 13 for Oahu. The distribution of SDB is generally in good agreement with the reference data for both Hateruma and Oahu. SDB for No. 12 appears noisy due to the effect of waves.

Manessa et al. (2016) also conducted accuracy verification using RF, and found the lowest RMSEs of 0.746 and 1.747 m in the two sea areas. Bathymetry data are mainly in the range of 0–10 m. They used WorldView-2 data, which has a 2-m resolution, and eight bands. Although their error is relatively small, an improvement in accuracy can be expected by combining our method. Ashphaq et al. (2021) reviewed > 100 papers on SDB. However, few studies used high-resolution images to obtain an RMSE < 0.5 m in the depth range of 0–10 m. This demonstrates the high accuracy of our results.

One of the problems with our proposed data selection method is that a more stringent threshold reduces the available data. The reduction in data not only affects model learning but also limits the scope of verification. The purpose of data selection is to exclude data from locations where the water depth changes rapidly, but it is necessary to confirm whether the distribution is as expected from images. Figure 3 shows the reference bathymetry selected by Method 2 for Hateruma.

It can be seen that data remain in areas where the water depth changes gradually. In such places, the bottom sediment is often sandy, so it is necessary to check whether other substrates, such as rocky areas, are also covered.

**Table 7.** Initial analysis results.

| No | Training Data (-5 ~ 25 m) | | Validation Data (0 ~ 20 m) | |
|---|---|---|---|---|
| | Number of data | RMSE (m) | Number of data | RMSE (m) |
| 1 | 361,032 | 1.57 | 36,095 | 2.10 |
| 2 | 1,242,870 | 2.53 | 422,439 | 2.45 |
| 3 | 361,032 | 1.29 | 36,095 | 1.85 |
| 4 | 1,242,870 | 2.42 | 422,439 | 1.87 |
| 5 | 300,803 | 0.99 | 37,756 | 1.38 |
| 6 | 479,100 | 1.59 | 176,010 | 1.41 |
| 7 | 300,803 | 0.80 | 37,756 | 1.21 |
| 8 | 479,100 | 1.45 | 176,010 | 1.29 |

**Table 8.** Second analysis results.

| No | Training Data (-5 ~ 25 m) | | Validation Data (0 ~ 20 m) | | Validation Data (0 ~ 10 m) | |
|---|---|---|---|---|---|---|
| | Number of data | RMSE (m) | Number of data | RMSE (m) | Number of data | RMSE (m) |
| 9 | 361,032 | 0.98 | 36,095 | 1.38 | 12,226 | 0.87 |
| 10 | 67,193 | 0.75 | 16,704 | 0.97 | 7,606 | 0.45 |
| 11 | 112,988 | 0.812 | 11,202 | 1.02 | 5,787 | 0.54 |
| 12 | 112,988 | 0.94 | 11,202 | 1.28 | 5,787 | 0.65 |
| 13 | 219,306 | 0.79 | 27,447 | 1.16 | 11,352 | 0.74 |

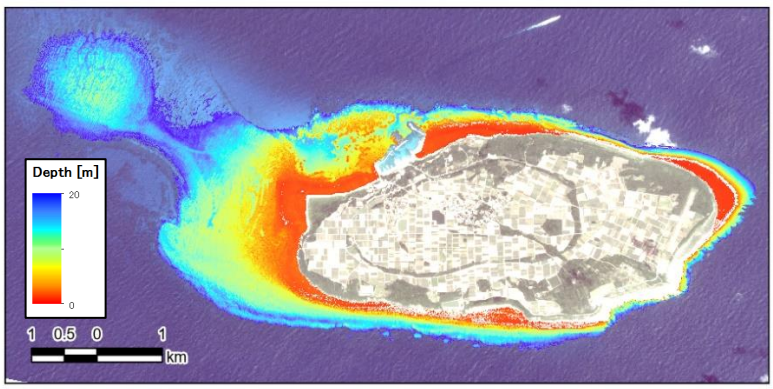


(a) Reference data for Hateruma

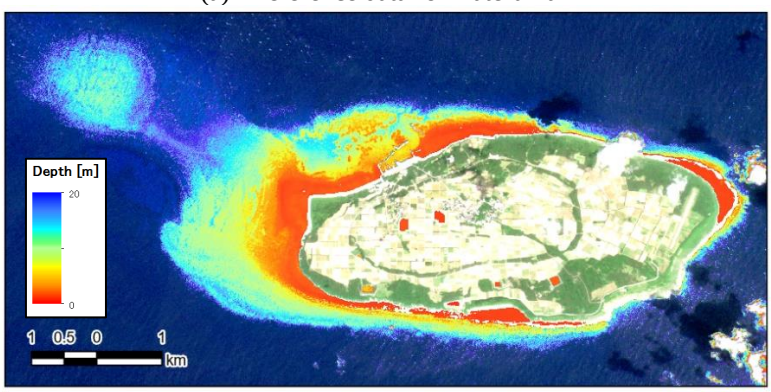


(b) SDB for Hateruma, Analysis No 10

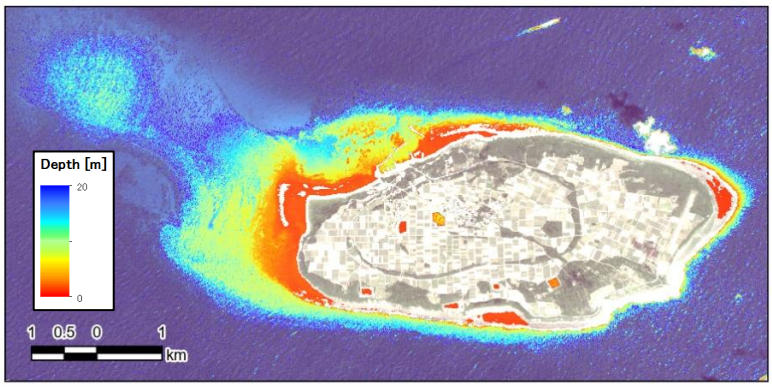


(c) SDB for Hateruma, Analysis No 12

Figure 1. Reference bathymetry data and SDBs for Hateruma from 0 to 20 m depth. PlanetScope images in 2017 and 2023 are used as background images for (a), (c) and (b), respectively.

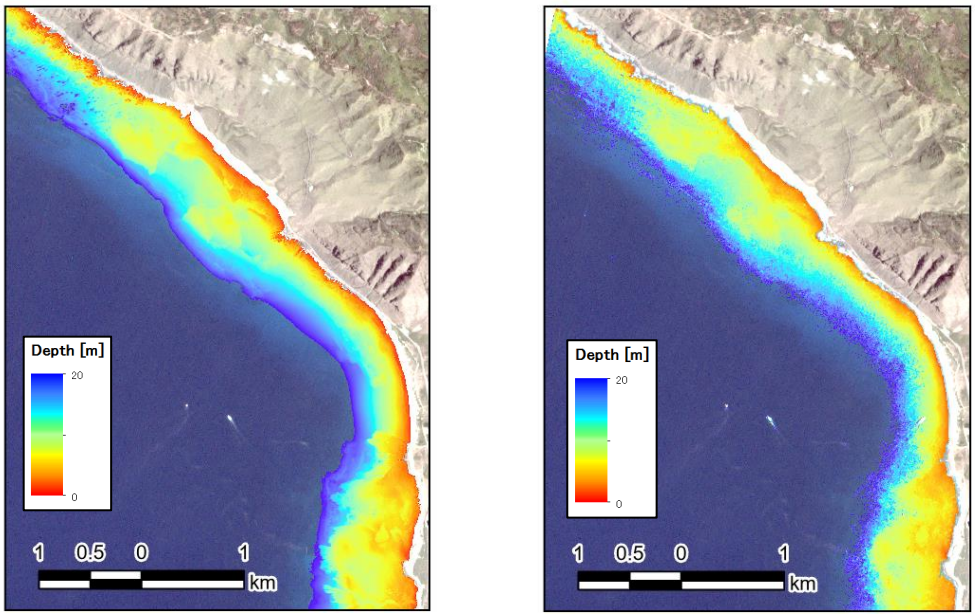


(a) Reference data in Oahu (b) SDB in Oahu, Analysis No 13

Figure 2. Reference bathymetry data and SDB for Oahu from 0 to 20 m depth. A PlanetScope image in 2017 is used as background image.

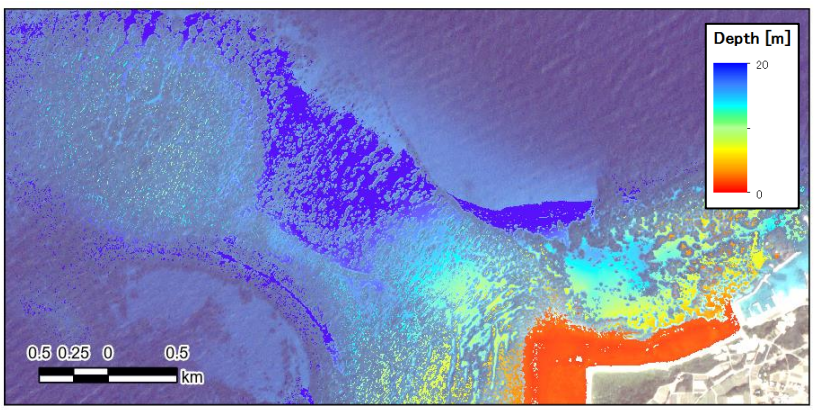


Figure 3. Reference bathymetry data selected by Method 2 for Hateruma. A PlanetScope image in 2017 is used as background image.

## 5. CONCLSION

We compared RF and DNN regression models for depth estimation, but there was little difference in terms of accuracy. Nevertheless, we were able to show that the error can be reduced by including surrounding pixels in the input data, increasing the number of bands, or selecting the training and validation data. The RMSE of SDB at Hateruma in the water depth of 0–10 m meets depth accuracy of A2 in ZOC, and the RMSEs in the range of 0–20 m meets depth accuracy of C in ZOC. The accuracy of ZOC A2 is sufficiently high, comparable to that of reference bathymetric data. The water depth estimation of SDB obtained by the method proposed here highly accurate compared with previous research.

## 6. ACKNOWLEDGEMENTS

Our acknowledgements to Planet Labs Education and Research Standard Program for providing us the PlanetScope imagery.

## 7. REFERENCES

Ashphaq, M., Srivastava, P.K., Mitra, D., 2021. Review of Near-Shore Satellite Derived Bathymetry: Classification and Account of Five Decades of Coastal Bathymetry Research. Journal of Ocean Engineering and Science, 6, 340–359, doi:10.1016/j.joes.2021.02.006.

International Hydrographic Organization, 2020. Mariners' Guide to Accuracy of Depth Information in Electronic Navigational Charts (ENC), Special Publication No. 67, Edition 1.0.0, International Hydrographic Organization, Monaco.

Lee, Z., Carder, K.L., Mobley, C.D., Steward, R.G., Patch, J.S., 1998. Hyperspectral Remote Sensing for Shallow Waters I A Semianalytical Model. *Applied Optics*, 37, 6329, doi:10.1364/AO.37.006329.

Lee, Z., Carder, K.L., Mobley, C.D., Steward, R.G., Patch, J.S., 1999. Hyperspectral Remote Sensing for Shallow Waters: 2 Deriving Bottom Depths and Water Properties by Optimization. *Applied Optics*, 38, 3831, doi:10.1364/AO.38.003831.

Lyzenga, D.R., Malinas, N.P., Tanis, F.J., 2006. Multispectral Bathymetry Using a Simple Physically Based Algorithm. *IEEE Transactions on Geoscience and Remote Sensing*, 44, 2251–2259, doi:10.1109/TGRS.2006.872909.

Manessa, M.D.M., Kanno, A., Sekine, M., Haidar, M., Yamamoto, K., Imai, T., Higuchi, T., 2016. Satellite-dreived bathymetry using random forest algorithm and WorldView-2 Imagery. *Geoplanning: Journal of Geomatics and Planning*, 3, 117, doi:10.14710/geoplanning.3.2.117-126.

Sagawa, T., Yamashita, Y., Okumura, T. and Yamanokuchi, T., 2019. Satellite derived bathymetry using machine learning and multi-temporal satellite images, *Remote Sensing*, 11, 1155, 1-19.